Thermal Underhood Analysis of a Heavy Commercial Vehicle Using Open Source CFD Package OpenFOAM

A Thesis

by

Çağatay Emre Ayhan

Submitted to the
Graduate School of Sciences and Engineering
In Partial Fulfillment of the Requirements for
the Degree of

Master of Science

in the
Department of Mechanical Engineering

Özyeğin University
January 2021

Thermal Underhood Analysis of a Heavy Commercial Vehicle Using Open Source CFD Package OpenFOAM

Approved by:

Asst. Prof. Altuğ Melik Başol,
Department of Mechanical Engineering
Özyeğin University

Asst. Prof. Özgür Ertunç,
Department of Mechanical Engineering
Özyeğin University

Assoc. Prof. Ayşe Gül Güngör,
Faculty of Aeronautics and Astronautics,
Department of Astronautical Engineering
İstanbul Technical University

Date Approved: 13.01.2021

To my family.

ABSTRACT

Underhood thermal design of heavy commercial vehicles has a large influence on the performance and reliability of the vehicles. Thermal design of underhood compartment is a challenging task with many constraints and design parameters. Designers can benefit from the numerical tools that are capable of predicting the thermal conditions inside the underhood area both accurately and fast. Conducting the design iterations using the numerical tools and conducting the experimental tests only for the final design would cut the vehicle design costs considerably. In this thesis, a numerical model for the underhood thermal analysis of a heavy commercial vehicle was developed using the open-source software OpenFOAM. OpenFOAM, is the most widely known open-source tool especially used for computational fluid dynamics and it is not much behind the commercial solvers in terms of capability.

In this study, the capabilities of OpenFOAM has been challenged on the underhood thermal analysis of a heavy commercial vehicle. The mesh generator *snappyHexMesh* performed fairly well in meshing of the complex geometries with reasonable resolution and quality. The *buoyantSimpleFoam* solver was used with the heat exchanger, rotating fan and heat shield models. The radiation heat transfer within the underhood area has been modeled using the surface-to-surface radiation model. The turbocharger heat shield temperature predicted with the solver matches reasonably well with the measurements with discrepancies less than 10ºC. Overall, the computational study took around 38 h running the solver on 56 CPU cores. Except the radiation model, the parallel scalability of the solver and the additional models were found to be close to

ideal. The radiation model takes about 1/3 of the overall computational time. The computational cost of the radiation model has been evaluated on different cases with varying number of surface elements involved in the radiation calculations. It has been found that, the computational cost of the radiation model strongly increases with the number of surface elements. In particular, using the radiation model with more than 20,000 surface elements does not seem to be computationally feasible due to the extreme computational cost of the model. This is partially due to the computational cost inherent to the surface-to-surface radiation model and, but it is also due to the lack of parallelization of the surface-to-surface radiation model in OpenFOAM version v1812+.

ÖZET

Ağır ticari araçların kaporta altı termal tasarımının araçların performansı ve dayanıklılığı üzerinde büyük etkisi vardır. Birçok sınırlamaya ve tasarım parametresine sahip olan kaporta altı termal tasarımı gerçekleştirmesi zor bir iştir. Bu bağlamda tasarımcılar kaporta altında hızlı ve doğru bir şekilde termal hesaplamalar yapabilen numerik araçlardan yararlanabilirler. Numerik araçlar kullanılarak yapılan tasarım iterasyonları ve sadece son tasarım için deneysel testlerin yapılması araç tasarım maliyetlerini önemli miktarda düşürebilmektedir. Bu tezde, bir ağır ticari aracın kaporta altı termal analizi için bir numerik model açık kaynak kodlu bir yazılım olan OpenFOAM kullanılarak geliştirilmiştir. OpenFOAM özellikle hesaplamalı akışkanlar mekaniğinde kullanılan ve en genel geçer bilinen açık kaynak kodlu yazılımdır ve kabiliyetleri bakımından diğer ticari yazılımların gerisinde de değildir.

Bu çalışmada, OpenFOAM yazılımının kabiliyetleri bir ağır ticari aracın kaporta altı termal analizi yapılarak test edildi. Mesh üreten bir araç olan snappyHexMesh komplex bir geometri olan kaporta altı için yeterli bir çözünürlükte ve kalitede mesh üretmede oldukça başarılı oldu. buoyantSimpleFoam çözücüsü ısı değiştiricileri, dönen fan ve ısı kalkanı modelleriyle birlikte kullanıldı. Kaporta altındaki radyason ısı transferi *yüzeyden yüzeye* radyasyon modeli kullanılarak modellendi. Çözücü sayesinde hesaplanan turbochargerın önündeki ısı kalkanı sıcaklığı ölçümlerle yeterli derecede eşleşiyordu; tutarsızlık 10 dereceden azdı. 56 işlemci çekirdeğiyle birlikte çalıştırılan çözücüyle koşturulan simulasyon toplamda 38 saat sürdü. Radyasyon modeli haricinde, çözücünün ve ek modellerin paralel ölçeklenebilirliğinin ideale yakın olduğu

görülmüştür. Toplam hesaplamalı zamanın üçte birini radyasyon modelinin hesaplanması oluşturmaktadır. Radyasyon modelinin hesaplama maliyeti, radyasyon hesaplamada kullanılan farklı sayıda yüzey elementine sahip caseler üzerinden değerlendirilimiştir. Yüzey elementi sayısı arttıkça radyasyon modelinin hesaplama maliyetinin şiddetli bir biçimde arttığı gözlemlenmiştir. Özellikle, 20,000'den fazla sayıda yüzey elementiyle yapılan radyasyon modellemesinin aşırı derecede büyük bir hesaplama maliyetine yol açmasından ötürü uygulanabilir olmadığı anlaşıldı. Bu kısmen yüzeyden yüzeye radyasyon modeline özgü hesaplama maliyetinden kaynaklanmaktadır. Aynı zamanda OpenFOAM v1812+'taki yüzeyden yüzeye radyasyon modeli hesabının paralelleştirilememesi de buna sebep olmaktadır.

ACKNOWLEDGMENTS

I am so grateful to Dr. Altug Basol for accepting me as his master student. It was a pleasant experience to work with him who has a positive and gentle personality. He motivated and encouraged me throughout the entire process of my research. He trusted me that I would do my best in my thesis research. I have learned a lot from him, and I am very grateful to him for his assistance in completing my thesis.

I am also so grateful to other members of thesis defence committee, Dr. Ozgur Ertunc and Dr. Ayse Gul Gungor, for their valuable comments and feedback on completing my work.

I especially thank my family for their endless support. Without their help, I would not have been able to complete this work.

TABLE OF CONTENTS

LIST OF FIGURES

LIST OF TABLES

CHAPTER I

INTRODUCTION

Modern heavy commercial vehicles are expected to operate reliably under harsh conditions. In this regard, especially in hot climates the thermal design of the underhood compartment plays an important role on the performance and reliability of the vehicle. However, the ever-increasing power requirements raise the thermal load onto the components at the underhood compartment. Modern heavy duty diesel engines can deliver power levels above 400 kW. The Center for Alternative Fuels, Engines & Emissions in West Virginia University have experimentally tested a heavy duty diesel engine and quantified the fuel energy conversion process into useful work and waste heat. Accordingly, a typical heavy duty diesel engine can convert 39.1% of the fuel energy into mechanical work. Meanwhile, 35.5% of the fuel energy is discharged through the exhaust as heat and around a total of 25% of the fuel energy is dissipated to the surrounding air by the water-cooling system and by the convective and radiative heat transfer from the surface of the engine components. Considering a 400kW diesel engine, this would mean that the engine discharges around 100kW heat into the underhood compartment of the vehicle. 70% of that heat is delivered into the underhood compartment by the heat exchangers and the remaining 30% of that is dissipated into air from the surface of the hot components. There are a number of heat dissipating components in the underhood compartment. Engine block has the largest surface area and it probably plays a dominant role in the overall heat transfer. However, due to the water cooling system its surface temperature does not go beyond the normal boiling point of water. So, it cannot cause an excessive temperature rise on the critical components such as electrical cables or on other type of heat sensitive parts. On the other hand, components that are connected to the exhaust gas line reach to temperatures up to 600ºC and they might cause excessive heating of the nearby components due to their high surface temperatures. The exhaust manifold, exhaust gas recirculation unit (EGR), turbocharger, exhaust pipes, and muffler are all positioned on the exhaust line and due to their high surface temperatures, the radiative transfer from their surfaces is quite considerable.

Thermal management of the underhood compartment is a challenging task. In one hand, providing excessive air flow into the tight and compact underhood compartment can keep the temperature of the components low, however it also increases the air drag on the vehicle. The so called cooling air drag acting on a passenger car has been measured by Kuthada and Wiedemann [1]. They have measured that the additional drag due to the cooling of the underhood compartment increases the drag coefficient of the vehicle by about 8-10%. On the other hand, reducing the air inflow into the compartment can keep the drag coefficient low but it also can lead to overheating of some engine components and thus lowers the reliability of the vehicle. In this regard, thermal design of the engine compartment has a critical role on the overall performance metrics of the vehicle.

In the modern engineering practice both the experimental and numerical methods are used in the underhood thermal design of heavy commercial vehicles. Carrying out real scale vehicle tests on large scale wind tunnels is very costly. Because of this reason, manufacturers are willing to benefit from the numerical techniques and to reduce the number of experimental tests as much as possible. However, accurate prediction of the underhood thermal conditions numerically is a challenging task. Unlike the aerodynamic calculations the error margin in heat transfer calculations can be quite large. The thermal conditions are dictated by the behavior of the thermal boundary layer at the wall. The accuracy of the heat flux or wall temperature predictions are heavily influenced by the mesh quality at the wall. However, reaching a high quality mesh at the wall might be difficult to generate due to the complexity of the geometry. In addition to that, radiation heat transfer also plays an important role in the heat load distribution. However, thermal radiation models have a large computational cost and they might dominate the overall computational cost of the numerical model.

In recent years, open-source numerical tools are gaining popularity. OpenFOAM, as the most widely known open source numerical package, was initially developed in 90's by Henry Weller. In 2004, it was released as an open source software by OpenCFD Limited founded by Henry Weller, Chris Greenshields and Mattijs Janssens. Later on, in 2012 OpenCFD Limited was acquired by the ESI Group and currently, the software is being developed and maintained by the ESI Group. There are other variants of OpenFOAM as well which all share the same code base. OpenFOAM, initially started to be used only in academia but in recent years also industry starts to show interest into it. The main advantage of the tool is that it is completely free to use. Secondly, the current capabilities of the tool are not much behind than the well-known commercial software such as Ansys Fluent, StarCCM+, or COMSOL. Moreover, due to the large user community of the tool, there is a large developer base which extend the capabilities of the tool continuously. However, due to the lack of graphical interface and documentation, switching from the commercial tool to OpenFOAM could still be problematic.

Underhood thermal analysis studies are computationally expensive. The computational domain is large and consists of hundreds of components. Moreover, heat transfer studies require a fine mesh resolution at the wall. In a typical underhood thermal analysis study the computational mesh may contain up to 100 million cells. In addition to that, radiation heat transfer between the components must also be taken into account.

Considering all these, one can see that the computational cost of the simulations can be quite high. In this regard, the parallel performance of the solvers and the models are quite important especially for the use in industry. OpenFOAM is a tool that is well tested on a variety of thermal studies and the parallel performance of the available solvers are at the level of commercial solvers.

In this study, the underhood thermal analysis of a heavy duty commercial vehicle has been conducted in OpenFOAM. The vehicle is designed and manufactured by Ford Otosan in Turkey. The vehicle shown in Figure 1 is given as a representative vehicle of the one studied in this work. Heavy commercial vehicles have different types and the one considered in this study is a tractor type. The trailer in the back is not considered in this study.

Figure 1 Tractor type heavy commercial vehicle designed by Ford Otosan representative of the one considered in this study

This thesis is organized as follows. In the literature survey part of this thesis, earlier studies related thermal underhood analysis are examined, and important findings are pointed out. In the methodology section, the details of the numerical model are discussed. Here, a special emphasis is given to the geometry preprocessing and mesh generation procedure since they impose a major challenge for the study. In the result section, first the convergence behavior of the model is analyzed and the air velocity and temperature field results in the underhood compartment are discussed. Next, the turbocharger heat shield temperature predicted with the use of the radiation model and flow solver is compared with the measurement data. Finally, the computational cost of the radiation model is discussed in detail.

CHAPTER II

LITERATURE SURVEY

One of the aims of the underhood thermal analysis conducted in early design development stage is to decrease design cycle time period and save cost. Karlsson et. al [1] have conducted a CFD analysis of the underbody of vehicle and succeeded to predict the thermal conditions in the vehicle underbody in close agreement with the experimental data. They also monitored temperature of the critical components exposed to excessive convective and radiative heat flux. Fuel tank is one of the critical components. They installed conventional and composite heat shields under the fuel tank and both installations satisfied the design requirements of the fuel tank.

One of the main studies on heavy vehicle underhood thermal analysis has been conducted by Nobel et al. [2] In this study, a numerical methodology was developed in order to conduct the underhood thermal analysis of a truck. They used the complete vehicle geometry in simulations. Their method is essential for both early design phase and post production phase of major truck programs. Ashmawey et al. [3] installed an underbody cover in order to decrease the environmental noise. However, it has been experimentally shown that installation of the underbody cover decreased the radiator air flow by around 6%. Chua et. al have studied [4] the cooling airflow around the engine compartment using 3-D simulations. Hountalas et al. [5] found that exhaust gas recirculation (EGR) cooling is beneficial for the heavy-duty diesel engine performance and emission. Especially, at high EGR rates and low engine speeds the need for EGR cooling was found to be more urgent. Tai et al. [6] and Alajbegovic et al. [7] have developed a numerical methodology that can predict radiator inlet cooling water temperature with a reasonable accuracy. Lam et al. [8] have conducted computational fluid dynamics simulations in order to determine the performance of the heat shields to reduce the maximum temperature of the engine components in the underhood region of a passenger vehicle. They have found that heat shields reduce the peak temperatures of the engine components by insulating the excessive heat from the engine block and from the exhaust and by regulating the airflow in the underhood compartment.

The positions of the components in the underhood area has a large influence on the thermal conditions inside the underhood area. In this regard, Gondipalle [9] has conducted two simulations with different radiator locations. In the first simulation, the radiator is located in front of the engine whereas in the second simulation the radiator is placed behind the engine. It has been observed that positioning the radiator behind the engine is harmful to the thermal behavior. They also stated that reaching the optimal position of the components in the underhood area is a time consuming and computationally expensive task. Maybe in future, simulation data can be used to generate reduced order models based on neural networks which later on might be used for the optimization of the underhood area.

Geometrical complexity of the components makes the geometry pre-processing step very challenging. Andra et al. [10] investigated the effect of simplifying the geometry of the engine compartment on the accuracy of the results. They have found out that geometrical simplification could be beneficial in evaluating different design alternatives in the early design stage. However, detailed engine geometry needs to be used when testing the final design alternatives. Engine geometry is a complex geometry, so generating meshes around engine geometry is difficult and costly. Katoh et al. [11] developed a mesh generation procedure to shorten the construction time of the simulation model. Flow and heat transfer analysis of the engine compartment were performed with simulations.

Radiation heat transfer plays an important role in the underhood area. Wendland [12] have found out that the radiation heat transfer is responsible for the 30% of the overall heat transfer at the engine manifold. Mao et al. [13] used the net radiation enclosure model [14] to calculate the surface-to-surface radiation heat transfer. They also came up with a numerical approach to speed up the convergence of the simulation. They have solved the air and solid domains separately in a segregated approach and thereby increased the convergence speed of the solver by a factor of 100.

Thermal soak studies have been conducted in [15] [16] [17]. Engine cooling jacket development and analysis has been done by Mulemane et. al [18]. Hallqvist et al. [19] numerically studied the required cooling air flows for the different designs of the engine, fan, heat exchangers and mesh screens. It has been proven that the distance between fan and radiator is a critical parameter affecting cooling air flow. Zyl [20] conducted a detailed study on vehicle underhood flow and thermal analysis. In order to reduce the computational cost of the problem, the effect of the cables and pipes on the flow and the thermal environment in the underhood area are neglected. The numerical results had a reasonable level of accuracy. Corbel [21] has developed a numerical method in which the water temperatures in the engine are calculated for different driving situations. Lawrence [22] conducted the underhood flow simulation to evaluate the influence of the fan on the air mass flow rate into the underhood compartment.

Due to the engine operation, temperatures at some of the vehicle component surfaces can increase dramatically. The rise in the temperature field can affect the velocity field by generating density variations in the air. Yang et al. [23] conducted thermal simulations implementing a coupled approach and they made a significant improvement in their underhood thermal results.

Fortunate et al. [24] have analyzed the shape of the air inlets on the heat transferred from engine and hot components. In this regard they evaluated the CFD results to increase the effectiveness of the air flow to improve the thermal management. Front end, underhood and underbody were modeled and analyzed separately in most of the studies before Damodaran's [25] study. This had a negative effect on the accuracy of the results. In addition, in many studies, the density of the air was considered constant. This also resulted in approximately 10 % errors. Damodaran's CFD analysis was one of the first studies that includes all the components including the radiator fan in a detailed way. They managed to reduce the modeling errors to around 5%. The flow predicted with the simulation correlated with test results to within 5%, while temperatures correlated to within 10% and 15%.

2.1 Studies Related Rotating Fan Models

Heavy commercial vehicles are equipped with powerful and large diameter fans. They have a dominant effect on the underhood thermal conditions. In this regard, the fan models used in the analysis have a considerable effect on the predictions. One of the most widely used fan models is the so-called multiple rotating frame (MRF) model. This approach is also known as the 'frozen rotor approach'. It is widely used in the modeling of rotating machinery, such as turbines, ventilators, and fans. In this method, the domain is divided into rotating and stationary zones. The rotating components of the fan are kept within the rotating domain where the flow equations are solved in the relative frame of reference. At the interface between the rotating and the stationary zones the flow variables are transferred keeping the rotating components fixed at a particular angular position.

This is a steady state model and computationally affordable in that sense. Reister et al. [26] has compared different fan models in terms of accuracy and computational cost. The models were multiple reference frame (MRF) approach, transient moving mesh and a body force approaches. It was found that the numerical simulation using the Multiple Reference Frame (MRF) model estimates the performance curve with a reasonable accuracy. The MRF model works with superior accuracy than the body force model and the MRF model is also computationally cheaper than the transient model. Both Gullberg et al., Sitong Ye, and Wang et al. used multiple rotating frame methodology in order to model the rotating fan and they both found that as MRF zone expands, accuracy of the results increases. [27] [28] [29] Especially as the size of the MRF region in the radial axis is decreased CFD method tends to underpredict the air mass flow rates. Gullberg et al. also conducted simulations in order to study the effect of the orientation of the stationary fan in the MRF model. Simulations have been done in which the fan was rotated 15 and 30 degrees, respectively. However, results did not change [30] . Jain et al. [31] conducted simulations resolving characteristics of the air flow through a radiator fan using CFD modelling. This study indicated that a CFD simulation could be extremely beneficial for estimating and understanding the flow distribution from a radiator fan for future research works.

2.2 Studies related to heat exchanger models

One of the important parts of the underhood geometry is the radiator. Its thermal and air flow behavior affect the thermal conditions in the underhood directly. In the last few years significant effort has been allocated to the development of numerical methods that will be able to lead the design of the cooling module and the underhood heat management of vehicles [3] [32] [4]. Fellague et al. [32] investigated the effect of air and temperature uniformity in the radiator inlet and they proved that the adverse effects of the nonuniformity in the inlet air velocity and temperature are small to the performance of the radiator. The effect of the flow nonuniformity on the sizing of the engine radiator was investigated by Chiou [33]. Radiator is one of the components which has a major effect on the thermal conditions inside the engine compartment. However, the fine geometrical details of the radiator would require mesh densities that would make the problem computationally prohibitive. Cetin et al. [34] have come up with a porous modeling approach and thereby have managed to reduce the radiator mesh size to only a few thousand cells. Sitong ye [29] conducted a study in which the whole car model is involved in order to simulate cooling air flow. In idle condition, radiator inlet mass flow rate was predicted with 20% error in comparison to the experimental results. Real heat exchanger geometries have not been used in the simulation. Instead, porosity model was used. Therefore, flow characteristics were not modeled precisely in heat exchangers. Moreover, in real wind tunnels there are more parts such as testing equipment and piping systems causing more details. Also, it is possible that experimental data has errors which cause more errors in the simulations. [29]

CHAPTER III

NUMERICAL METHODOLOGY

For the thermal analysis of the underhood components of the vehicle a three-dimensional CFD analysis has been conducted. In this section, the main steps of the numerical methodology are discussed starting with the preprocessing stage. Next, the governing equations and the solver settings are specified alongside with the boundary conditions. Finally, the details of the important numerical models such as heat exchanger, thermal radiation, and heat shield are explained.

3.1 Geometry Preprocessing

Underhood compartments of modern heavy commercial vehicles contain thousands of components that are tightly clustered around the engine. Some of the main components in the underhood compartment are engine block, gearbox, heat exchangers, fan components, pipes, cables, exhaust manifold, muffler, pipes, heat shields. The complex geometry of those components makes the preprocessing stage very challenging. This stage requires a combination of different tools. For the geometry preprocessing the utilities of the StarCCM+ software have been used. The "surface repair" tool is used to close the holes on the geometry. To reduce the number of the surface patches, patches that are in contact are combined and assigned as a new combined patch. "Surface wrapper" utility is executed to ensure that the closed geometries are airtight. This utility also prevents problems during the surface remeshing process. The "surface wrapper' utility requires around 5 min run time for a target surface mesh size of 1cm. Here, it is important to point out that the “surface wrapper” utility has not been used with the baffle type geometries such as heat shields since it adds an artificial thickness to the geometries. Finally, the “surface remeshing” utility is used, and the geometry is ready to be used by the mesh generator.

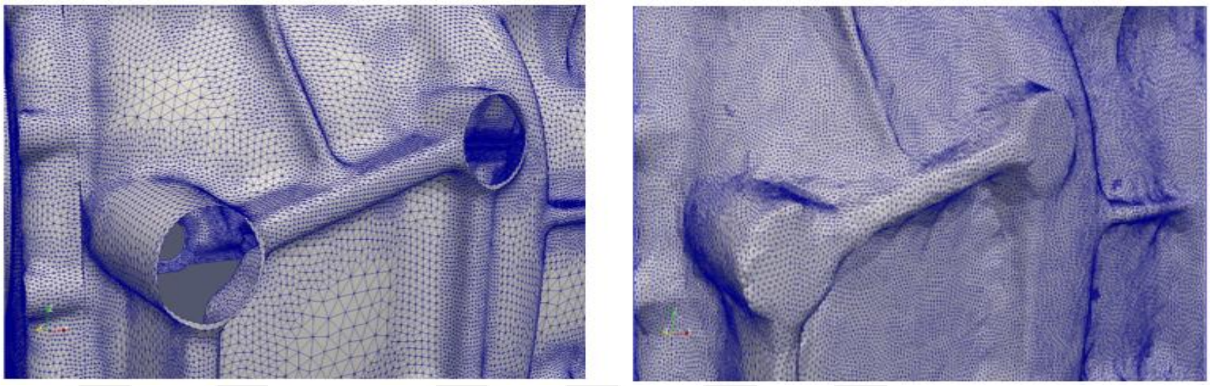

Figure 2 View of the engine surface - before preprocessing (left) and after geometry preprocessing (right)

3.2 *Mesh Generation*

For the mesh generation, the open source mesh generator *SnappyHexMesh* was used. This is one of the mesh generators available in OpenFOAM. It generates an unstructured, hexahedral type mesh and is preferred for the meshing of complex geometries such as the components in the underhood compartment. The mesh generator is also capable to add prism layer cells to resolve boundary layers. As a first step in the mesh generation process, the exported geometry files preprocessed with StarCCM+ are converted into *.stl* format using the “*surfaceMeshConvert*” utility. The mesh generator initially requires a uniform cartesian background mesh which will be refined at the boundaries according to the desired resolution. Figure 3 shows the computational domain around the vehicle. The dimensions of the domain are 32.0 m in length, 10.2 m in width and 7.1 m in height.

Length, width and the height of the truck is 5.5 m, 2.45 m and 3.7 m respectively. Distance between front end of the truck and the inlet of the computational domain is 8.81 m. So, the length of the computational domain is 3.6 times higher than the distance between front end of the truck and the inlet of the computational domain. The truck is in the middle of the width of the computational domain. The width of the computational domain is approximately 4 times higher than the width of the truck. The distance between top of the truck and upper wall of the computational domain is 1.99 m, and height of the domain is 3.6 times higher than the distance between top of the truck and the upper wall.

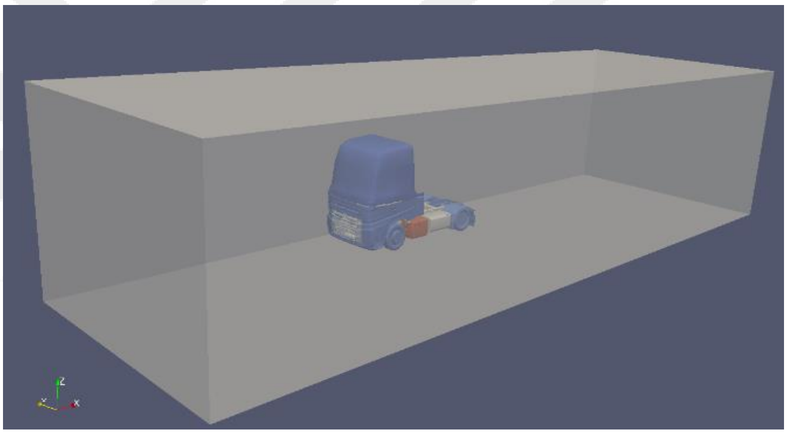

Figure 3 Computational Domain

The background mesh was generated with the "*blockMesh"* utility with a uniform cell size of 20cm. It resulted to a mesh with about half a million cartesian cells. The background mesh and the refinement boxes are shown in Figure 4 and in Figure 5. The cell sizes at the boundary of the important components are provided in Table 1. To keep the mesh skewness low, a castellated mesh type was used around the solid boundary of most of the engine components. This has the advantage to keep the cell skewness and aspect ratio low and results in high mesh quality at the boundary. Since most of the engine components do not have aerodynamically smooth surfaces, the effect of the modifications in the solid boundary due to the castellation process is rather low.

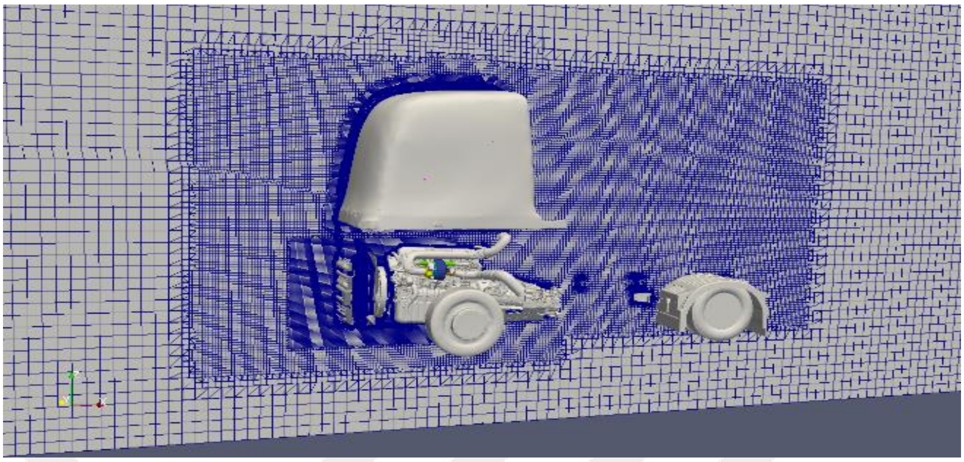

Figure 4 Mesh refinement boxes around the engine compartment and cabin

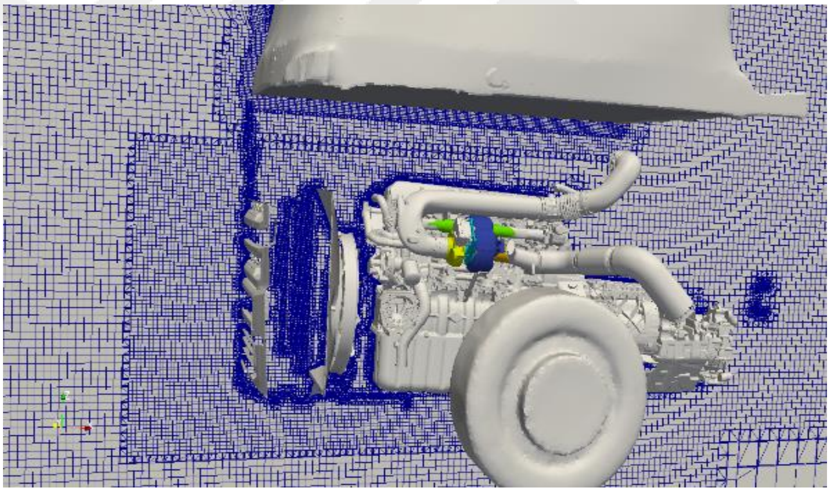

Figure 5 Underhood mesh

Table 1 Some important underhood compartments and their surface mesh resolutions

Heat exchangers surface	6.25 mm
Grill	1.6 mm
Fan blade	1.6 mm
Engine block	3.125 mm
Exhaust manifold	3.125 mm
Exhaust pipe	6.25 mm
Turbocharger heat shield	3.125 mm
Turbocharger	1.6 mm

3.2.1 Heat exchanger mesh

Heat exchangers have a dominant effect on the thermal conditions of the underhood compartment. The engine is equipped with 3 heat exchangers. These are the main heat exchanger, intercooler, and the condenser of the air conditioning unit. Due to their complex geometry, carrying out a high-fidelity flow analysis around heat exchangers would be computationally very expensive. Because of this reason, the heat exchangers are modeled as porous media which only requires a uniform cartesian mesh inside the heat exchangers. In this regard, a separate refinement box has been generated for each of the three heat exchangers using *snappyHexMesh*. Next, the associated cell zones have been marked with the *topoSet* utility. Additionally, it is also required to specify the inlet face zones. They are required for the mass flow rate calculations. The mesh generated for the heat exchangers is shown in Figure 6.

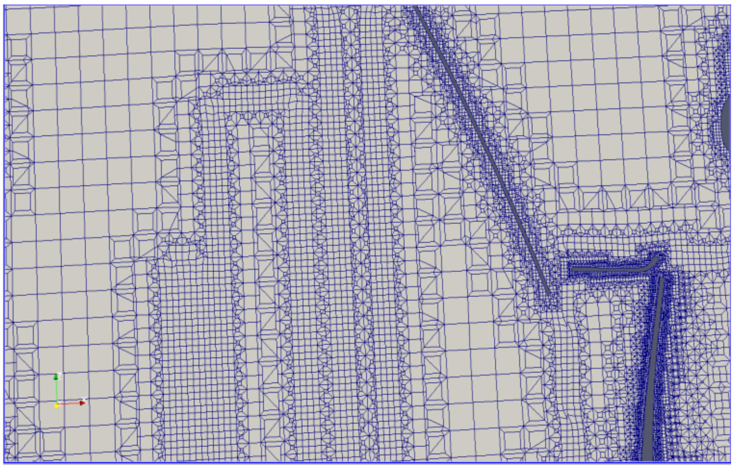

Figure 6 Mesh zones for the radiators

3.2.2 Fan Mesh

Especially at low speeds the convection through the underhood compartment is forced by the fan mounted right downstream of the heat exchangers. The fan operates at high rotational speeds and the aerodynamic smoothness of the blades have a huge impact on its performance. Therefore, a body fitted mesh type was used around the fan blades. According to the preliminary study, using a castellated mesh type resulted in a large error in the prediction of the cooling air mass.

3.2.3 Cabin Mesh

The cabin of the vehicle has a direct effect on the aerodynamics of the vehicle. Moreover, it also affects the thermal conditions in the underhood compartment. The blockage created by the cabin generates a low pressure zone in the back of the cabin which helps to increase the mass flow through the underhood compartment. Therefore, it is critical to accurately capture the flow physics especially at the back of the cabin. To be able to capture the flow features at the back of the cabin, the boundary layer at the top of the cabin must be accurately resolved. For this reason, whole cabin geometry is separated into “upperCabin” and “lowerCabin” parts using StarCCM+. Initially, a body fitted mesh was generated on the upper cabin surface. The body fitted mesh can sometimes lead to small artificial irregularities on the surface which can disrupt the flow in the boundary layer. To prevent that, the snap tolerance value was set to 3 for the upper cabin surface. Effect of the snap tolerance value on the surface geometry representation can be seen in Figure 7. This feature is especially important if prism layer cells are to be used at the wall to resolve the viscous boundary layers. Adding prism layers on irregular surfaces usually results in poor mesh quality in many cases and it even leads to failure in the mesh generation process. Boundary layer mesh was added only for the upper cabin surface. Expansion ratio was set to 1.2 and the final layer thickness was set to 1 cm. The prism layer generated on the cabin surface is shown in Figure 8.

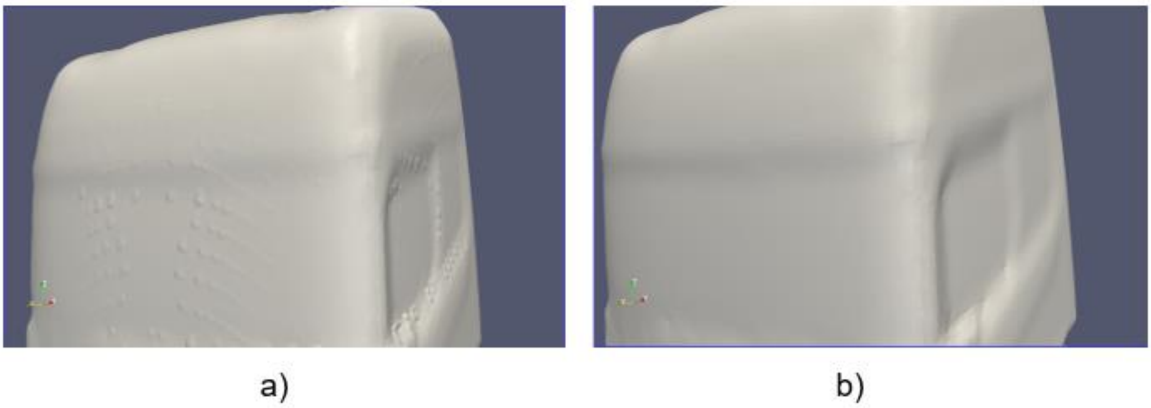

Figure 7 Reconstructed cabin surface with the snap tolerance value set to a) 1.5 and b) 3.0.

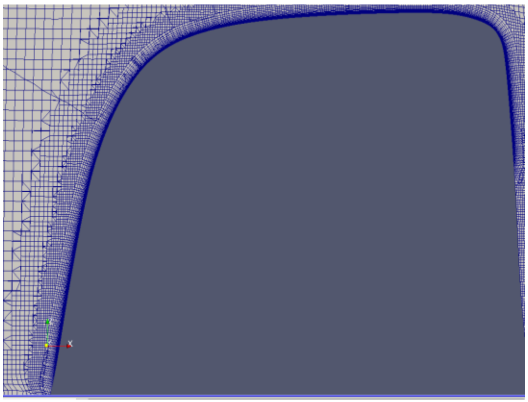

Figure 8 Prism layer mesh to resolve the boundary layer on the cabin

3.2.4 Heat shield mesh

Heat shields are basically thin layers of metals used to block the radiation emitted from hot surfaces. They are made of double layered metals with the insulation material in-between the layers. Since the heat shields are extremely thin, the heat conduction within the heat shield can be modeled using a one-dimensional heat conduction model. However, the mesh around the heat shield still needs refinement to resolve the boundary layers on the wall. For this reason, the zones around the heat shields were refined during the mesh generation process by *snappyHexMesh*. Then *createBaffles* utility was used to generate baffles from the .stl files. The turbocharger heat shield mesh is shown in Figure 9.

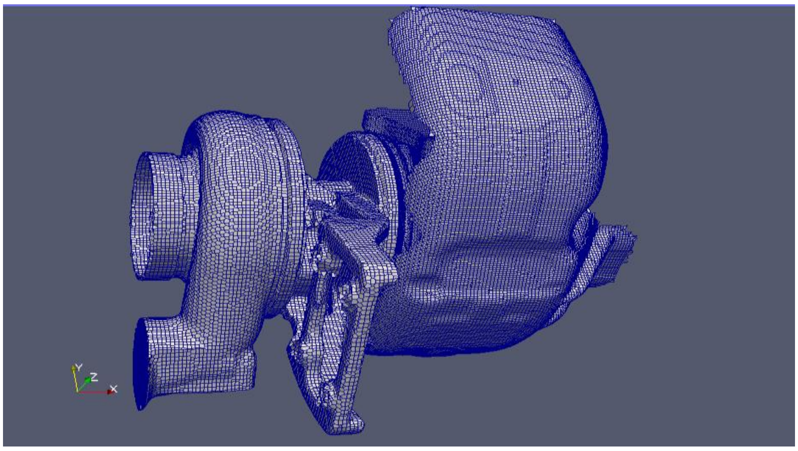

Figure 9 Turbocharger and the heat shield surface mesh

3.3 Solver

For this thermal study the *buoyantSimpleFoam* solver in OpenFOAM version v1812+ has been used. It is a steady state solver developed for the modeling of turbulent, compressible flows. Thanks to its compressible nature, it accounts for the density variations due to heat transfer. The solver also has an interface with different turbulence models and with different thermal radiation models present in OpenFOAM library. In this study, the turbulence has been modelled with the two equations turbulence model k-ω SST.

3.3.1 Numerical schemes

In this solver the momentum and the energy equations are solved in a segregated manner using the SIMPLE algorithm. [8] As a particular feature of this scheme, under-relaxation factors are required for the stability. They have large influence on the convergence behavior. On one hand, using relaxation factors close to 1 may lead to divergence and on the other hand, setting them close to 0 can significantly reduce the convergence rate of the solver. In this study, the relaxation factors for the momentum and pressure equations were set as 0.8 and 0.2 respectively. Before running the solver, an appropriate initial guess was generated using the potential flow solver in OpenFOAM. This prevents the solver from crashing, but it also helps with the convergence speed.

3.3.2 Boundary conditions

At the inlet of the domain the air velocity, temperature and flow directions were specified and at the outlet static pressure was provided as boundary conditions. Additionally, the turbulence intensity and eddy viscosity ratio were specified at the inlet. No detailed information was available about the turbulence conditions at the inlet. In this study, turbulence intensity at the inlet was taken as 7.5% and the eddy viscosity ratio was set to 10. The inlet boundary conditions are tabulated in Table 2. The side, top and bottom walls of the computational domain were modelled as slip walls. No slip boundary conditions were imposed at the surfaces on the vehicle. Due to the lack of the boundary layer mesh, wall function approach was used for the modeling of the turbulent boundary layers. Regarding the energy equation, the components are classified into three groups about the type of boundary conditions used.

i. Parts with adiabatic temperature boundary conditions
ii. Parts with known temperature boundary conditions
iii. Parts with radiation heat flux boundary conditions

Table 2 Inlet boundary conditions

Inlet Air Velocity	28.2 km/h
Inlet Air Temperature	38.2 ºC
Inlet air turbulence intensity	7.5 %
Inlet eddy viscosity ratio	10

3.4 Component Models

3.4.1 Heat exchanger model

Heat exchangers play a dominant role in the engine cooling and have a major influence on the thermal conditions in the underhood compartments. Due to their complex geometry it is computationally extremely expensive to calculate the heat transfer without using macroscopic models. In this study, heat exchangers have been modeled using porosity models. Darcy Forchheimer model [35], one of the porosity models in OpenFOAM, calculates the blockage due to the heat exchanger by adding a sink term in the momentum equations and a source term in the energy equations. In this model the momentum sink terms are calculated as shown in the equation below.

$$S_m = -\mu DU - \frac{1}{2}\rho tr(U.I)FU \qquad (1)$$

Table 3 Porosity coefficients set in the simulation for radiator, intercooler and condenser

Radiator	
D coefficient	(5981462.1 598146210 598146210)
F coefficient	(166.5 16650 16650)

Intercooler	
D coefficient	(16611382.9 1661138290 1661138290)
F coefficient	(105.5 10550 10550)

Condenser	
D coefficient	(40471211.7 4047121170 4047121170)
F coefficient	(92.0 9200 9200)

Here, the porosity coefficients D and F are to be provided in the *fvOptions* file using manufacturer's data. Three values in a row represent coefficients in the x,y and z axis respectively. Due to the orientation of the fins inside the radiators air can only flow parallel to the fins and not sideways. Accordingly, the porosity coefficients in the y and z directions are set to very large numbers. In addition to that, effectiveness tables, secondary mass flow rate, secondary flow temperature were also provided to the model for each of the 3 heat exchangers. During the calculations the heat rejection rate into air was monitored for all the heat exchangers and compared with the experimental data as an indicator for the reliability of the computational results.

3.4.2 Fan model

In this study, the so-called multiple rotating frame approach (MRF) was used for the modeling of the fan. In this approach, the fan is modelled in the rotating frame of reference and the stationary components such as the casing around the fan is modeled in the stationary frame of reference. The data between the domains is transferred during the computations. The rotational speed of the fan was set to 1063.9 rpm.

3.4.3 Heat shield model

Heat shields are used to block the thermal radiation emitted from the hot components. They are basically thin double layer sheets made of aluminum and with insulation material between the layers. The emissivity of the layers, the internal conductivity across the layers and their total thickness are set in the simulation settings. Imposing the measured temperature of the turbine casing of the turbocharger and solving for all the heat transfer modes (radiation, 1D solid conduction and convection) the surface temperature of the inner and outer heat shield walls have been calculated and compared with the measurements to validate the computational model.

3.5 Radiation Heat Transfer Model

Radiation heat transfer plays an important role on the surface temperature of high temperature components such as exhaust manifold, turbocharger, muffler and it also increases the surface temperature of the components nearby the thermal radiation sources. The radiative heat flux reaching to temperature sensitive components such as cables or pipes can cause serious damage. Because of these reasons, radiation effects must be incorporated into the underhood thermal models. Air surrounding the underhood compartments can be considered as a nonparticipating medium. Air acts almost completely transparent to the radiation emitted by the hot surfaces. Due to this particular nature of the problem, radiation effects can be calculated using the surface-to-surface radiation model. OpenFOAM is equipped with the surface-to-surface radiation model that calculates the radiation heat fluxes on the selected surfaces using the net radiation method. [14] This method treats the surfaces as opaque, grey and diffuse surfaces.

In this method, first the view factors between the surfaces are calculated in a preprocessing step. View factors are basically geometrical factors representing the amount radiation energy emitted from one surface A_1 and intercepted by the other surface A_2 as shown in Figure 10.

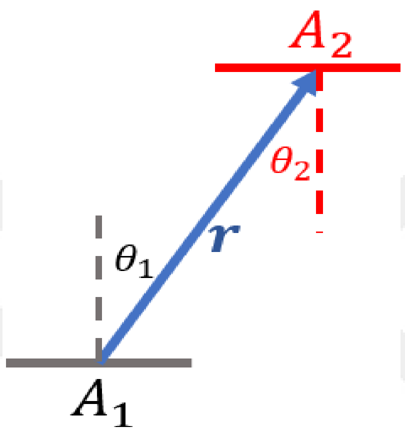

Figure 10 View factor between two surfaces with areas A_1 and A_2

View factors between any finite surfaces are calculated as

$$F_{A_1 \to A_2} = \frac{1}{A_1} \int_{A_1} \int_{A_2} \frac{\cos(\theta_1)\cos(\theta_2) dA_1\, dA_2}{\pi r^2} \tag{2}$$

Following the same approach for each cell on the surface, one can calculate the view factors between every surface cells. However, the integrals are approximated by evaluating the integrand only for the cell centers. Calculating the view factors between every surface cell is a computationally costly procedure and the computational cost scales with the 2nd power of the number of surface cells considered. So, doubling the number of surface cells results in a 4x increase in the computational time. In addition to that, after calculating the view factors they have to be stored on a square matrix of size NxN where the N is the total number of surface cells considered in the view factor calculations which is also memory intensive since the matrix is not necessarily sparse.

Next, using the view factors the conservation of radiation energy between the surfaces is expressed in a linear system as shown in equation (3).

$$Cq = b \tag{3}$$

$where$

$$C_{ij} = \left[\frac{\delta_{ij}}{\epsilon_j} - \left(\frac{1}{\epsilon_j} - 1\right) F_{ij}\right] \tag{4}$$

$$b = \sum_{j=1}^{N} \left[\delta_{ij} - F_{ij}\right] (E_b)_j \tag{5}$$

In the linear system above, the emissivity of the surfaces is taken into account in the matrix C on the left hand side and the temperature of the surfaces is considered on the right hand side vector b. The resulting radiative heat fluxes on the surface cells can be calculated by solving the linear system. Usually, these linear systems can be large in real engineering calculations and the associated computational cost can be huge. Moreover, the linear system has to be solved every time the temperatures of the surface cells change. However, the change in the surface temperature does not alter the matrix C, but only modifies the right-hand side vector b. Under these conditions, factorization of the matrix C into a lower (L) and upper (U) triangular matrices such that LU = C would bring a huge speed up when the same linear system has to be solved multiple times but each time with different right hand side vectors. Following this approach, OpenFOAM spends a considerable amount of computational in the first iteration for the LU decomposition of the left hand side matrix but this pays later on off with the reduction in the computational time for the solution of the heat flux vector every time the radiation model is called.

For the use of the surface-to-surface radiation model in OpenFOAM, one has to first define the surfaces participating in the radiation transfer and the view factors between the surface has to be calculated beforehand. Here, as discussed before, instead of using the same fluid mesh for the radiation heat transfer calculations one may also agglomerate the faces and calculate the view factors between the agglomerated faces later on. This would reduce the number of faces involved in the radiation heat transfer calculations and thereby the computational cost would be reduced. Next, the formed linear system shown in Eq 1 has to be decomposed in the first iteration and in the subsequent iterations the decomposed linear system has to be used to solved for the required heat fluxes.

In this study, the radiation heat transfer calculations were conducted to calculate the surface temperature of the turbocharger heat shield and the predictions were compared with the measurements. To do that, the temperatures of the surrounding radiation emitting surfaces have to be specified. In this study two different cases are considered in terms of the surfaces participating in the radiation calculations. In Case 1, apart from the heat shield, the turbocharger, part of the exhaust manifold and only the initial section of the exhaust pipe were considered. (Figure 11) In addition to that, the emissivities of the surfaces were also specified alongside. Except at the heat shield, the temperature of the other radiation emitting surfaces were specified. At the heat shield surface, the net radiative heat flux and the heat conducted across the layers are considered and the resulting surface temperatures were calculated. In Case 2, the number of surfaces involved in the radiation calculation was increased. In Case 2, in addition to the components specified in Case 1, the entire exhaust pipe and exhaust manifold and exhaust gas recirculation (EGR) system were included in the radiation calculations. (Figure 12).

In both Case 1 and Case 2 the radiation model were used with the agglomeration of surface cells. Even though this approach is very useful in reducing the computational cost of the model, it could lead to serious errors when used too aggressively. In this regard, the same scenario considered in Case 2 was repeated in Case 3. However, the agglomeration of the surface cells was considerably reduced as compared to Case 2. The total number of agglomerated surface cells participating in the radiation calculations are given in Table 4.

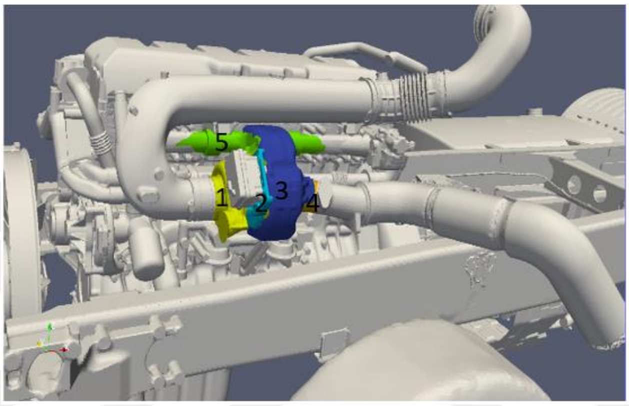

Figure 11: Surfaces which are involved in radiation calculation are shown in color – Case 1

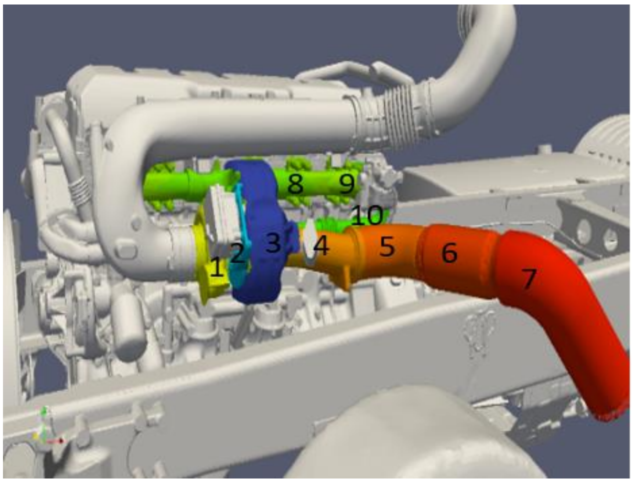

Figure 12: Surfaces which are involved in radiation calculation are shown in color – Case 2 and 3

Table 4 Number of agglomerated surface elements involved in the radiation calculations for Case 1, 2 and 3

CASE NUMBER	# OF SURFACE ELEMENTS IN RADIATION CALCULATIONS
1	6440
2	11200
3	19010

3.6 Postprocessing

In underhood thermal analysis studies of vehicles one usually has to deal with large data sets. So, downloading the entire data set at once and conducting the post-processing on the entire data set could not be possible on standard desktop computers. OpenFOAM has utilities that can only extract the required 2D or 3D data from the entire flow field data. OpenFOAM’s *setSet*, *boxToCell* and *subsetMesh* utilities were used for this purpose. In OpenFOAM, *boxToCell* is a tool under *setSet* utility. *boxToCell* utility generates boxes in aimed sections of the domain and selects the computational cells inside the box. Next, selected cells were converted into *polyMesh* format using *subsetMesh*. In this study the results were postprocessed using this technique. In addition, foamToVTK utility was used to generate surface data. For instance, turbocharger surface temperature results were generated using foamToVTK utility. Thanks to *noInternal* feature of the foamToVTK tool, it was possible to extract only surface fields.

CHAPTER IV

RESULTS

The details of the computational model have been mentioned in the previous section. Simulations have been conducted with the developed numerical model and with the boundary conditions taken from the measurements. In this section, first the convergence behavior of the computational model is going to be discussed and next, the velocity and temperature fields in the underhood compartment will be given. A particular emphasis is given on the calculation of the heat shield temperature attached to the turbocharger casing. There, the effect of the thermal radiation is highly important and it is modelled with the surface-to-surface radiation model. The calculated heat shield surface temperature has been compared with the measurements. Finally, the computational costs of the main solver, each of the component models and especially of the radiation model have been evaluated.

4.1 Convergence Behavior

To reduce the computational cost of the simulation a stepwise procedure has been followed for the activation of the different models. In this regard, the first 4000 iterations had been conducted without activating the heat exchanger, fan and radiation heat transfer models. Next, the heat exchanger models had been switched on, and the simulation was kept running for an additional 1000 iterations. After that, the rotating fan model was activated and the simulation was kept running for an additional 2000 iterations. Finally, the radiation model was also activated for the last 3000 iterations. Overall, 10,000 iterations have been conducted. Figure 13 shows the residual history of the simulation. The spikes at certain iteration numbers are due to the activation of the models.

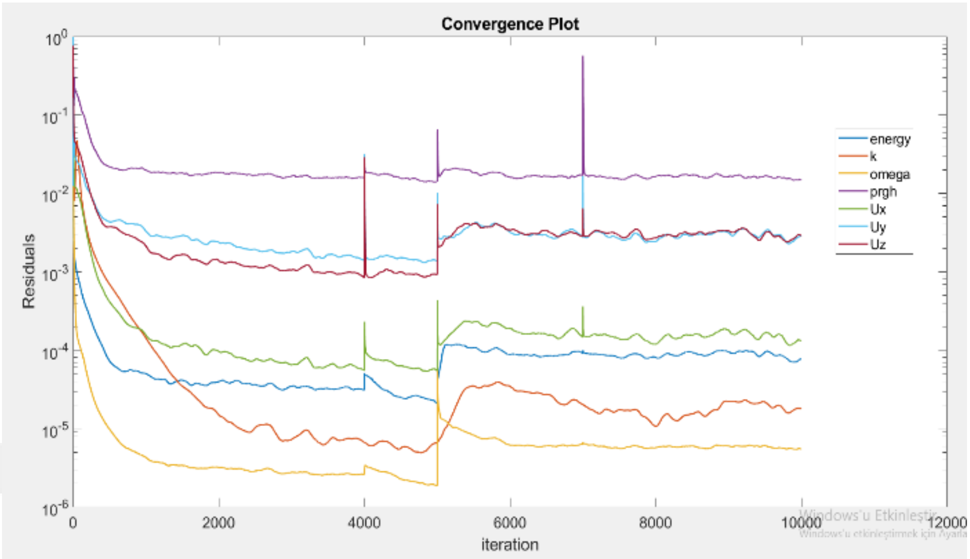

Figure 13: Residual history

In addition to the residuals, the calculated heat rejection rates of the heat exchangers were also being monitored during the computations as shown in Figure 14. As discussed before, the heat exchanger models were activated after 4000 iterations had been conducted with the base solver. However, since the fan was kept nonrotating for the next 1000 iterations after the activation of the heat exchanger models the heat rejection rates were quite low. Once the fan rotation is turned on, the heat rejection rates increased to their realistic values. As shown in Table 5, the heat rejection rates of the heat exchangers were predicted close to the measurements. Numerical predictions underestimated the heat rejection rate from the radiator and intercooler by about 5% and 12% respectively.

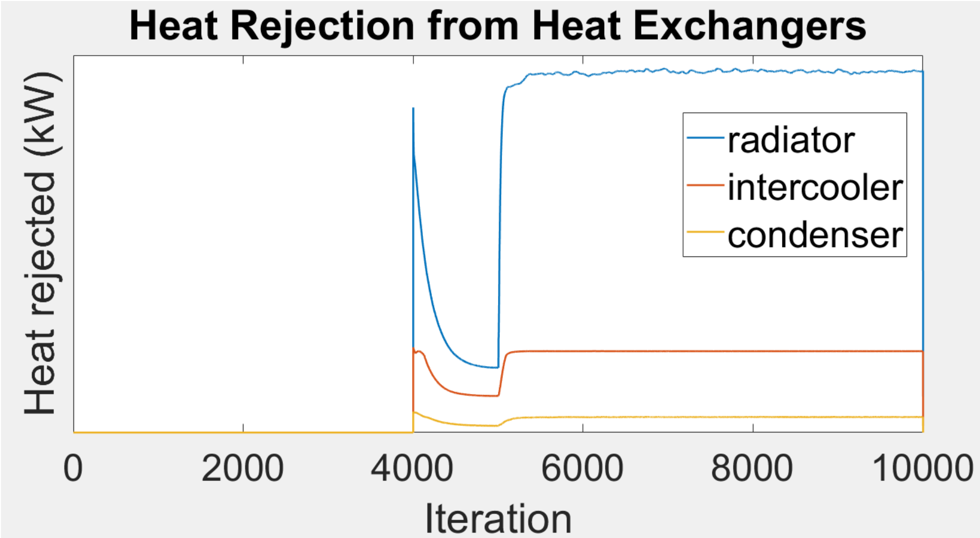

Figure 14 Heat rejection rate vs. iteration number

Table 5 Relative error in the predicted heat rejection rates based on measurements

	Relative Error in Heat Rejection Rate
Heat rejection from radiator	5 %
Heat rejection from intercooler	12 %

4.2 Air Velocity and Temperature

The u-velocity field around the vehicle is shown in Figure 15. There is a large circulation zone at the back of the cabin. The low pressure zone generated by the cabin helps to drive the flow through the underhood compartment and increases the cooling effectiveness at the expense of additional air drag. In addition to that, the rotating fan mounted on the front of the vehicle forces the air flow through the underhood compartment. A close view to the velocity field around the engine is given in Figure 16. The air that is forced by the fan migrates radially outward due to the swirl in the flow. The air temperature field at the cross-section of the underhood compartment is given in

Figure 17. As shown, the temperature downstream of the heat exchangers reaches to 393 K. This data is provided by the manufacturer as a boundary condition to simulate the extreme conditions that the vehicle can face with. The hot air discharged into the underhood compartment mixes out with the cold air on the way out from the underhood compartment. Figure 18 shows the air temperature distribution below the engine block. As shown here, the high temperature air discharged from the fan quickly mixes out with the cold air. The resulting mixture penetrates the entire region underneath the vehicle.

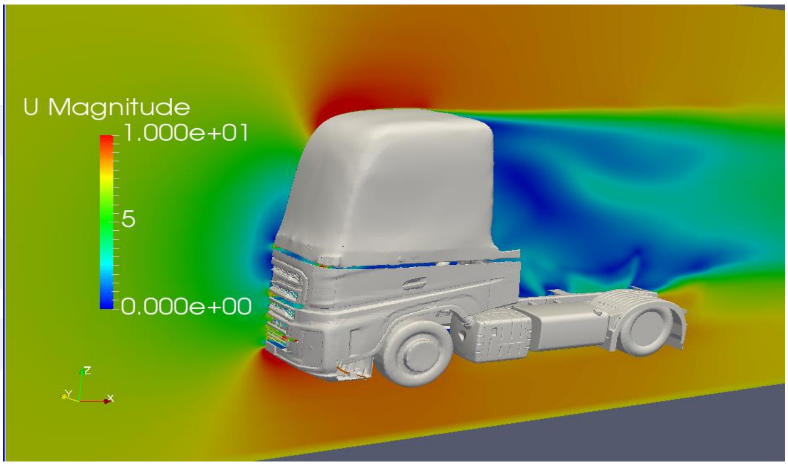

Figure 15: x-component of the velocity field [m/s]

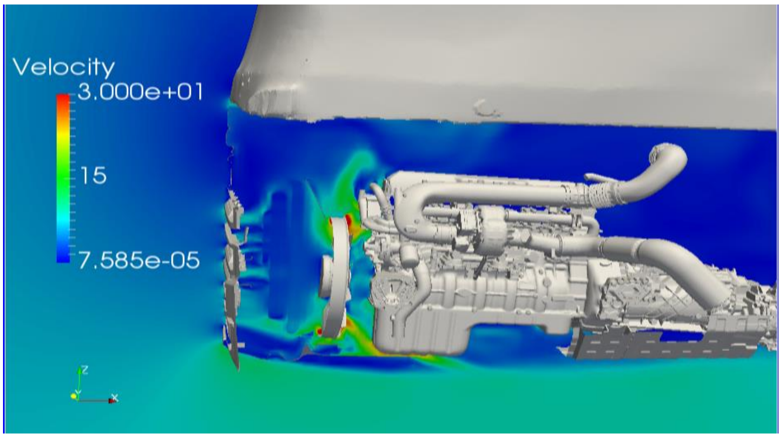

Figure 16 x-component of the velocity field [m/s]

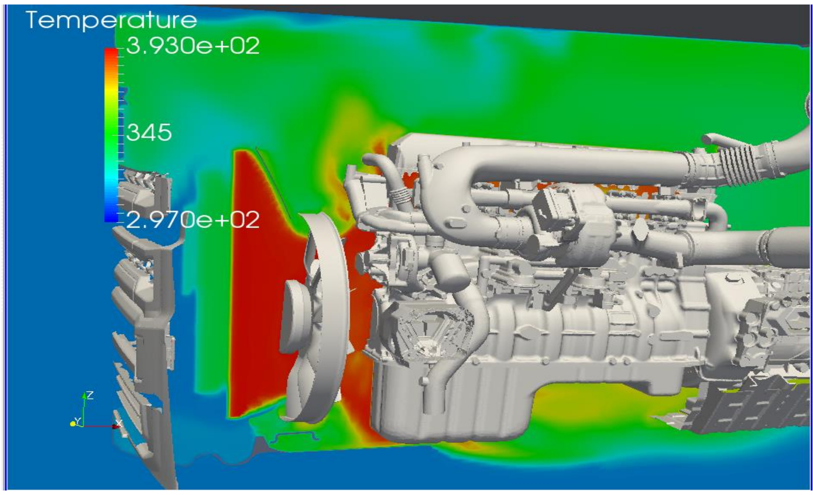

Figure 17 Air temperature field around the engine [K]

Air entered from the inlet grills reach the heat exchangers and is heated up in here. Heated air flows through the rotating fan and conveyed through the underhood and increases the overall temperature of the air in the underhood. This may lead to excessive surface temperatures in the critical zones where temperature sensitive components are located. This heat load might damage the temperature sensitive components in such zones. Methods of preventing excessive heating of this components can be installing flow routers in the critical zones in order to direct the flow away from the critical components or installing heat shields in front of the thermally sensitive components.

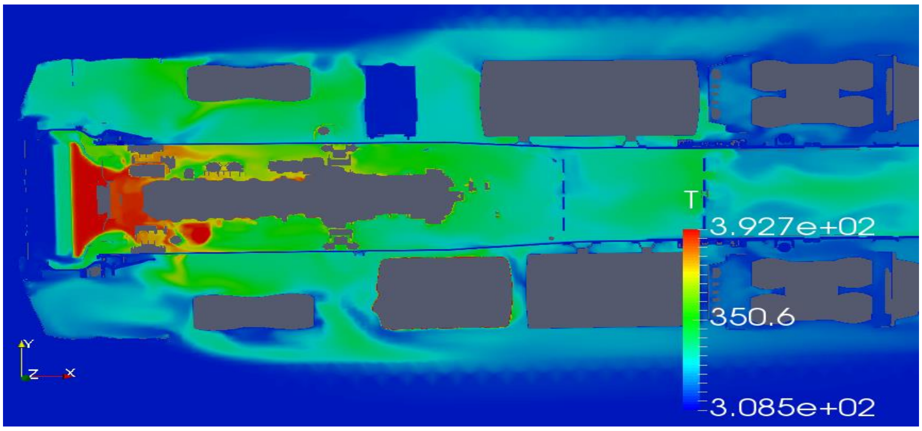

Figure 18 Air temperature field underneath of the vehicle [K]

4.3 *Turbocharger Heat Shield Temperature*

The turbocharger is used to increase the pressure of the air directed to the engine intake. The work required to compress the air is extracted by the turbine from the enthalpy of the exhaust air. Because of that, the turbine is placed right at the outlet of the exhaust manifold and has to withstand temperatures as high as 600ºC. At these temperature levels heat transfer by thermal radiation is quite considerable and can lead to the overheating of the nearby heat sensitive components. To prevent that, heat shields are placed around the turbocharger. Even though heat shield can block the direct radiation emitted from the turbine casing, eventually it also heats up and starts to emit thermal radiation. However, due to the high reflectivity of the heat shield its emissive power is a lot less. However, it still has a considerable effect on the temperature of the nearby components.

Figure 19 shows the predicted temperature distribution on the outer layer of the heat shield for the two sets of calculations conducted with different number of surface patches included in the surface-to-surface radiation model. In Case 1, only the exhaust manifold, the turbocharger turbine and its heat shield were included in the radiation heat transfer calculations. In Case 2, the exhaust pipe up to the connection point with the muffler was also considered in the radiative heat transfer calculations. As shown in Figure 19, both simulations predict similar average temperature levels on the heat shield. However, the surface temperature predicted with Case 2 is slightly higher than that of Case 1 especially on the left hand side of the shield. This is an expected result since the surfaces of the exhaust pipes also emit thermal radiation and thereby contribute to the heating of the heat shield.

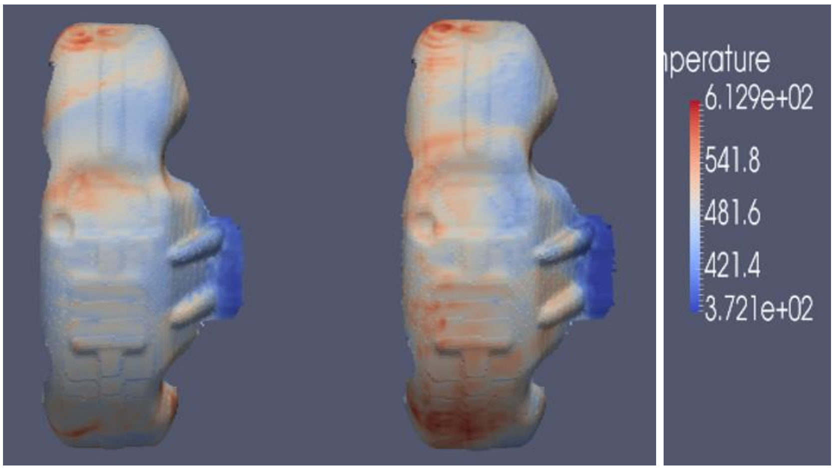

Figure 19 Turbocharger heat shield outer wall temperature [K] – Case 1 (left) and Case 2 (right)

As discussed before, the computational cost of the surface-to-surface radiation model is highly dependent on the number of surface elements involved in the radiation calculations. Often, to reduce the computational cost of the surface-to-surface radiation model the mesh that is used in the flow calculations is coarsened and the radiation calculations are carried out on that coarser level mesh and the calculated heat fluxes are mapped back onto the flow mesh. This procedure is called face agglomeration. However, even though this procedure can provide a huge saving in computational time it might also create considerable errors if it is used too aggressively. Figure 20 shows the temperature distributions on the heat shield calculated by using different level of face agglomeration. The temperature distribution on the left hand side belongs to Case 2. The solution on the right hand side, Case 3, is obtained by using a less aggressive face agglomeration technique. As shown, the predictions are similar, however there are also local temperature differences between the two.

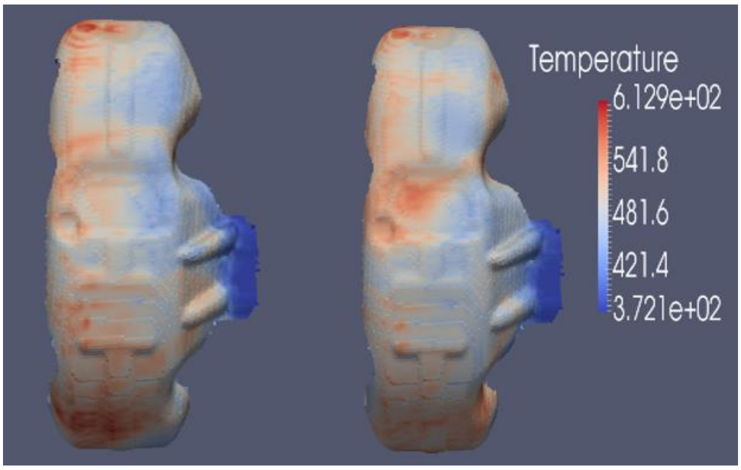

Figure 20 Turbocharger heat shield outer wall temperature [K] – Case 2 (left) and Case 3 (right)

Finally, the temperature predictions of Case 1 are compared with the readings of the local temperature sensors distributed over the outer layer of the heat shield. Those measurements have been provided by the industrial partner. Table 6 shows the predictions and measurements at the sensor locations on the heat shield. As shown, the agreement is quite satisfactory with errors less than 10ºC.

Table 6 CFD vs Measurement of heat shield local temperatures

Sensor No	CFD	Measurement
1	462 K	466 K
2	482 K	486 K
3	508 K	515 K

4.4 Computational Cost

Lastly, the computational cost of the simulations is going to be discussed. The simulations were conducted on the computer cluster at Ozyegin University. The computational cost of the simulations and the parallel scalability of solver have been evaluated running the computations on 28 and 56 Intel Xeon E5-2680 v4 CPU cores. The computational time required for a single iteration are given in Table 7 for the base solver and for the additional models used. As shown, adding the heat exchanger and rotating fan models do not show a considerable increase in the computational time. The effectiveness of the parallelization of the base solver and of the models were tested by comparing the computational times of the simulations on 28 and 56 CPU cores. As shown, doubling the number of CPU cores reduces the computational time of the base solver by nearly a factor of two which shows that the effectiveness of the parallelization is almost ideal at these number of cores used. Since, the computational cost of the additional models except the radiation model is negligible, evaluating the parallel scalability of these model were not possible in this study. Next, the computational cost of the radiation model was evaluated for Case 1. As shown in both simulations conducted either with 28 or 56 cores, the surface-to-surface radiation model leads to a major increase in the computational time. This is partially associated with the computational cost of the surface-to-surface radiation model. However, the dominant effect in the rise of the computational cost is due to the lack of the parallelization of the surface-to-surface radiation model in OpenFOAM version v1812+. As shown, increasing the number of CPU cores does not reduce the computational cost of the radiation model. So, running the simulation even on higher number of cores brings diminishing returns in overall speed up.

Table **7** Computational cost of the convection solver and the additional cost of the models running on 28 and 56 CPU cores

	Run time / iteration (on 28 cores)	**Run time / iteration (on 56 cores)**
Convection only	22.0 s	11.3 s
Convection + Heat exchanger models	22.0 s	11.5 s
Convection + Heat exchanger models + Rotating fan model	22.2 s	11.5 s
Convection + Heat exchanger models + Rotating fan model + Radiation model (Case 1)	27.8 s	17.9 s

As mentioned before, the increase in the computational time per iteration with the surface-to-surface radiation model is quite substantial. However, the radiation model also requires other preliminary steps which all need to be conducted before starting with the iterations. Those preliminary calculation steps are the view factor calculations and LU decomposition of the linear system of equations. The computational costs of these preliminary calculation steps have been evaluated on Cases 1, 2 and 3. As opposed to the heat flux calculations which need to be conducted every time the radiation model is called by the solver, these preliminary calculations have to be conducted only once. As shown in Table 8, the computational costs of all the different calculation steps heavily increase with the number of surface elements. Starting with the view factor calculation step, it is the only one that is parallelized. View factor calculations for each surface element can be calculated independently from the others and because of this reason, it is a very suitable algorithm for parallelization. Theoretically, the computational time for the view factors calculations scales with the 2nd power of the number of surface elements. So, increasing the number of elements by 2x should result in a 4x increase in the computational time.

However, the measured rise in the computational time exceeds this theoretical value. This issue could not be related to the shared use of the cluster since the view factor calculations were run using the entire number of cores on the 2 nodes of the cluster. So, it must have been related to the implementation of the algorithm. Next, the computational cost of the LU decomposition stage is going to be evaluated. As shown in Table 8, the LU decomposition is computationally the most costly preliminary step. This is partially due to the lack of parallelization in the implementation but it also is inherently computationally more intensive in comparison to the view factor calculation. Moreover, theoretically the computational cost of the LU decomposition algorithm scales with the 3rd power of the number of the surface elements. The rise in the computational time observed in Cases 1,2 and 3 are approximately in line with the theoretical value.

Table 8 Computational cost of the calculation steps of the surface-to-surface radiation model in OpenFOAM

Case	**# of agglomerated surface elements**	**View Factor (56 cores)**	**LU Decomp. (single core)**
1	6,440	10 s	840 s
2	11,200	60 s	4440 s
3	19,010	300 s	26640 s

CHAPTER V

DISCUSSION AND CONCLUSION

Even though there is a growth in electric passenger vehicles market, replacing the combustion engines with the electric motors in heavy commercial vehicles does not seem to be possible in the near future. In this regard, the thermal design of the underhood compartment is important both in terms of performance and reliability of the heavy commercial vehicles. However, designing the underhood compartment of the vehicle is a challenging task with many constraints and design parameters. In that sense carrying out the design iterations using computational techniques is a lot more economical than conducting measurements in road tests or wind tunnels. In this study, a numerical model has been developed and applied for the underhood thermal analysis of a heavy commercial vehicle. The vehicle has been designed by Ford Otosan in Turkey.

In this study, the thermal analysis of the vehicle has been conducted using the open-source software OpenFOAM. It has been mostly used for computational fluid dynamics and currently it has reached to a large user base all around the world. Even though the tool has reached to a decent maturity level, using it on flow simulations as challenging as this one is still not straightforward. Underhood thermal analysis is a challenging problem mostly because of its geometrical complexity. Generating a mesh with the required mesh resolution at the boundary layers and also keeping the cell skewness low is a difficult task to manage. In this regard, the *snappyHexMesh* tool in OpenFOAM performs reasonably well in the mesh generation process. It has the capability of generating a castellated or body-fitted mesh and it can also add prism layers to resolve the boundary layers. The fact that it is equipped with these options is very handy when dealing with the complex geometries. Switching to castellated mesh type on regions where the geometry is highly complex is sometimes the only option that the solver can work with. However, one should also point out that the surfaces need to be well prepared before starting with the mesh generation. StarCCM+ is quite capable in that aspect and was used in the geometry cleaning and processing stage.

The solvers in OpenFOAM give the user the flexibility to choose from a wide range of discretization schemes. Especially for meshes where the mesh quality can not be above a certain level, switches to increase the robustness of the solvers is a must. In this regard, the discretization schemes for convective fluxes in OpenFOAM give the users the flexibility to adjust the robustness and accuracy of the solver by limiting the 2nd order fluxes according to the user input. Additionally, OpenFOAM is also equipped with component models that are required by the underhood thermal analysis. The heat output rates from the heat exchangers are compared with the measurement data and showed an agreement with less than 5% error in heat transfer rate.

In thermal analysis the radiation heat transfer plays a considerable role too. In this study, the radiation heat transfer was dealt with the surface-to-surface radiation model because air does not participate in the radiation transfer. Using the radiation model the turbocharger heat shield temperatures were calculated and the predicted temperatures were in agreement with the measurement data with discrepancies less than 10ºC. Additionally, the computational cost of the radiation model were evaluated on three different cases with varying number of surface elements. The computations have emphasized the computational cost of the radiation model. This is partially due to the inherent computational cost of the method, but it is also due to the lack of parallel implementation of the surface-to-surface radiation model in the OpenFOAM version v1812+ that is used in this thesis.

Overall, the developed model is able to predict the turbocharger heat shield temperature in close agreement with the measurements. Except the radiation model, all the models and the solver are parallelized and shows a close to ideal scalability. The surface-to-surface radiation model is currently not parallelized which heavily limits its use. Scenarios with more than 20k surface elements are hardly feasible in terms of computational cost.

BIBLIOGRAPHY

[1] R. Karlsson, P. V. Benthem and M. Islam, *Vehicle Underbody Thermal Simulation Using Computational Fluid Dynamics*, Detroit: SAE International, 1999.

[2] T. P. Nobel, *A Multi-Dimensional Approach to Truck Underhood,* Chicago: SAE International, 2001.

[3] M. Ashmawey, H. Berneburg, W. Hartung and F. Werner, *A Numerical Evaluation of the Thermal Effects of the New V6 Engine on the Underhood Environment of the 1993 Opel Vectra*, Detroit: SAE International, 1993.

[4] K. Chua, A. J. Bilanin and M. E. Olson, *Engine Compartment Heat Rejection Analysis via Navier-Stokes Simulations,* Detroit: SAE International, 1993.

[5] G. C. Mavropoulos, K. B. Binder and D. T. Hountalas, *Effect of exhaust gas recirculation (EGR) temperature for various EGR rates on heavy duty DI diesel engine performance and emissions,* Zografou: National Technical University of Athens, 2006.

[6] C. H. Tai , C. G. Cheng and C. Y. Liao, *A Practical and Simplified Airflow Simulation to Assess Underhood Cooling Performance,* Detroit: SAE International, 2007.

[7] A. Alajbegovic, W. Jansen and J. Amodeo, *Thermal Management Simulation for Passenger Cars - Towards Total Vehicle Analysis,* 2006.

[8] S. Lam, N. Shuaib, H. Hasini and N. Shuaib, *Computational Fluid Dynamics Investigation On the Use of Heat Shields for Thermal Management in a Car Underhood*, International Journal of Automotive and Mechanical Engineering, 2012.

[9] S. r. Gondipalle, *CFD Analysis of the Underhood of a Car for Packaging Considerations,* All Theses, 2011.

[10] R. Andra, E. Hytopoulos, K. Kumar and R. L. Sun, *The Effect of Boundary and Geometry Simplification on the Numerical Simulation of Front-End Cooling,* Detroit, Michigan: SAE International, 1998.

[11] N. Katoh, T. Ogawa and T. Kuriyama, *Numerical Simulation on the Three Dimensional Flow and Heat Transfer in the Engine Compartment,* SAE Technical Paper, 1991.

[12] D. Wendland, *Automobile Exhaust-System Steady-State Heat Transfer,* SAE International, 1993.

[13] S. Mao, Z. Feng and E. Michaelides, *Off-highway Heavy-duty Truck Under-hood Thermal Analysis,* Applied Thermal Engineering, 2010.

[14] J. Howell, M. Menguc and R. Siegel, *Thermal Radiation Heat Transfer, sixth edition,* 2015.

[15] Minovski, Lofdahl and Gullberg, *Numerical Investigation of Natural Convection in a Simplified Engine Bay,* SAE Technical Paper, 2016.

[16] B. Sweetman, I. Schmitz, B. Hupertz, N. Shaw and J. Goldstein, *Experimental and Numerical Investigation of Vehicle Drive and Thermal Soak Conditions in a Simplified Engine Bay,* SAE International, 2017.

[17] B. Minovski, L. Löfdahl, J. Andric and P. Gullberg, *A Coupled 1D–3D Numerical Method for Buoyancy-Driven Heat Transfer in a Generic Engine Bay,* MDPI, 2019.

[18] A. Mulemane and R. Soman, *CFD Based Complete Engine Cooling Jacket Development and Analysis,* Rosemont: SAE International, 2007.

[19] H. Thomas , *The Cooling Airflow of Heavy Trucks – a Parametric Study,* SAE International, 2008.

[20] J. M. V. Zyl, *Numerical Modeling and Experimental Investigation of the Flow and Thermal Processes in a Motor Car Vehicle Underhood,* Stellenbosch University, 2006.

[21] J.-C. Corbel, *An Original Simulation Method for Car Engine Cooling Systems: A Modular System,* SAE Technical Paper, 1987.

[22] V. Lawrence, *Underhood Airflow Simulation of a Passenger Car Using Computational Fluid Dynamics,* Brasil: SAE Technical Paper, 2001.

[23] Z. Yang, J. Bozeman and F. Z. Shen, *Thermal-velocity Coupling in Vehicle Thermal System Calculations,* Detroit: SAE Technical Papers, 2002.

[24] F. Fortunato, F. Damiano, L. D. Matteo and P. Oliva, *Underhood Cooling Simulation for Development of New Vehicles,* Toronto: SAE International, 2005.

[25] V. Damodaran and S. Kaushik, *Simulation to Identify and Resolve Underhood/Underbody Vehicle Thermal Issues,* Fluent Inc, 2000.

[26] H. Reister and F. Ross, *Numerical Simulation of an Axial Cooling Fan,* SAE Technical Paper, 1997.

[27] A. Wang, Z. Xiao and H. Ghazialam, *Evaluation of the Multiple Reference Frame (MRF) Model in a Truck Fan Simulation,* Toronto: SAE International, 2005.

[28] P. Gullberg, L. Löfdahl , S. Adelman and P. Nilsson, *An Investigation and Correction Method of Stationary Fan CFD MRF Simulations,* SAE International, 2009.

[29] S. Ye, *Prediction of Airflow for Automotive Cooling Applications Using OpenFOAM,* Ontario: University of Windsor, 2018.

[30] P. Gullberg, L. Löfdahl, S. Adelman and P. Nilsson, *A Correction Method for Stationary Fan CFD MRF Models,* SAE International, 2009.

[31] S. Jain and Y. Deshpande, *CFD Modeling of a Radiator Axial Fan for Air Flow Distribution,* International Journal of Mechanical and Mechatronics Engineering, 2012.

[32] K. A. Fellague, S. H. Hu and D. A. Willoughby, *Determination of the Effects of Inlet Air Velocity and Temperature Distributions on the Performance of an Automotive Radiator,* Detroit: SAE International, 1994.

[33] J. P. Chiou, *The Effect of the Flow Nonuniformity on the Sizing of the Engine Radiator,* Detroit: SAE Technical Papers, 1980.

[34] B. Çetin, K. Güler and M. H. Aksel, *Computational Modeling of Vehicle Radiators Using Porous Medium Approach,* Bilkent University, 2017.

[35] "https://openfoamwiki.net/index.php/DarcyForchheimer," [Online].

VITA

Cagatay Emre Ayhan has completed his B. Sc. degree in mechanical engineering from Bogazici University in 2017. He started his M. Sc. degree in mechanical engineering under the supervision of Assistant Professor Altug M. Basol in Ozyegin University. His main research interest is vehicle underhood thermal analysis.